

Zero-Shot Image Harmonization with Generative Model Prior

JIANQI CHEN, YILAN ZHANG, ZHENGXIA ZOU, KEYAN CHEN, and ZHENWEI SHI, Beihang University, China

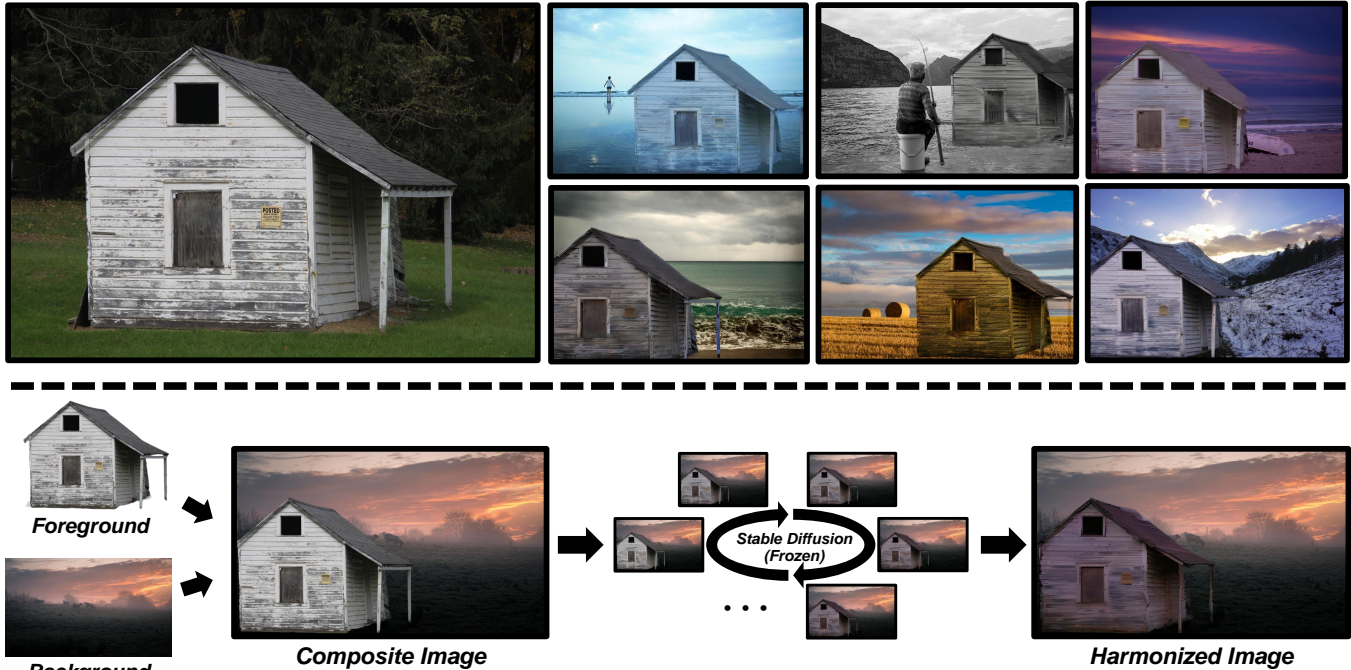


Fig. 1. Given a composite image, our method can achieve its harmonized result, where the color space of the foreground is aligned with that of the background. Our method does not need to collect a large number of composite images for training, but only utilizes pretrained generative models. The first column from the left in the upper row is the source image of the foreground (“house”), and the others are the harmonized results of the foreground object in different backgrounds. In the lower row, we take one of the composite images as an example to show the harmonization process. For a concise overview of our approach, please refer to our **presentation video**: <https://www.youtube.com/watch?v=mfbTIVp6JBU&t=4s>.

We propose a zero-shot approach to image harmonization, aiming to overcome the reliance on large amounts of synthetic composite images in existing methods. These methods, while showing promising results, involve significant training expenses and often struggle with generalization to unseen images. To this end, we introduce a fully modularized framework inspired by human behavior. Leveraging the reasoning capabilities of recent foundation models in language and vision, our approach comprises three main stages. Initially, we employ a pretrained vision-language model (VLM) to generate descriptions for the composite image. Subsequently, these descriptions guide the foreground harmonization direction of a text-to-image generative model (T2I). We refine text embeddings for enhanced representation of imaging conditions and employ self-attention and edge maps for structure preservation. Following each harmonization iteration, an evaluator determines whether to conclude or modify the harmonization direction. The resulting framework, mirroring human behavior, achieves harmonious results without the need for extensive training. We present compelling visual results across diverse scenes and objects, along with a user study validating the effectiveness of our approach.

Github Code: <https://github.com/WindVChen/Diff-Harmonization>

1 INTRODUCTION

Image harmonization is a technique for aligning the color space of foreground objects with that of the background in a composite

image. Recent state-of-the-art methods [Chen et al. 2023c; Cong et al. 2022; Guo et al. 2022; Ke et al. 2022; Liang et al. 2022; Sofiiuk et al. 2021; Xue et al. 2022; Zhan et al. 2020] are mostly based on deep learning networks which have achieved more promising results than traditional ones [Lalonde and Efros 2007; Pitie et al. 2005; Reinhard et al. 2001; Sunkavalli et al. 2010; Xue et al. 2012]. However, the performance of these methods, either performing image harmonization in a supervised manner with paired inharmonious/harmonized images [Chen et al. 2023c; Cong et al. 2022, 2020; Guo et al. 2022; Hang et al. 2022; Jiang et al. 2021; Ke et al. 2022; Tsai et al. 2017; Xue et al. 2022] or constructing a zero-sum game by means of GAN [Goodfellow et al. 2014] technique [Chen and Kae 2019; Zhan et al. 2020], is highly correlated with the quality of the collection of composite images. If the collected composite images could not cover real-world situations, then the trained network will fail to obtain satisfactory results in practical use.

Compared to curating a collection of natural images, creating a real-world composite image entails higher labor costs. This involves extracting a foreground object from one image and seamlessly integrating it into another at an appropriate location. To mitigate the impractical cost associated with constructing a large real composite

image dataset, prevailing methods [Chen and Kae 2019; Cong et al. 2020; Tsai et al. 2017] opt for the “synthesis” of composite images. This is achieved by applying diverse color transformations [Fecker et al. 2008; Lee et al. 2016; Pitié et al. 2007; Reinhard et al. 2001; Xiao and Ma 2006] to the semantic regions of extensive segmentation datasets [Bychkovsky et al. 2011; Lin et al. 2014; Zhou et al. 2019]. These transformations yield “synthesized” composite images along with their paired harmonized counterparts (*i.e.*, the originals). While incorporating more transformations improves proximity to the distribution of real-world composite images, it also results in a substantial dataset [Cong et al. 2020], imposing a heavy burden during training. In this paper, we contend that such a resource-intensive approach diverges from typical human behavior.

Let’s consider how humans harmonize a composite image. 1) First, we quickly identify the possible imaging environment of the foreground and the background regions, including factors such as time of day, season, and added color tones. 2) Next, we mentally visualize the foreground’s appearance in the background’s imaging condition and utilize basic controls in image editing software, such as Photoshop, to edit the foreground accordingly. 3) After each round of editing, we pause to evaluate the result, determining whether it has achieved harmonization. If successful, we conclude the process; otherwise, we consider refining the current direction. This process doesn’t necessitate human training on large datasets of inharmonious images and operates in a zero-shot manner. We attribute its success and feasibility to humans’ strong prior understanding of what a natural image should entail. Specifically, most of our observations in our lives are of natural and harmonious scenes, influencing our tendency to imagine and create harmonious compositions. Therefore, the harmonization process is to gradually bring an initial outlier (inharmonious composite image) closer to our established prior (illustrated in Fig. 2). There is no need to understand the distribution of composite images. This concept finds strong support in early human cognitive research [Biederman et al. 1982] and [Davenport and Potter 2004], which demonstrated humans’ rapid and accurate perception of inconsistencies between objects and backgrounds in scenes. This underscores humans’ innate ability to harmonize visual elements, forming the theoretical foundation of our approach.

To emulate human behavior, we identify four key components in the human harmonization process: human reasoning (identifying imaging conditions for foreground and background), human prior regarding natural image appearances, image editing software for operations, and continual intermediate evaluation for adjustments. Drawing inspiration from the advancements in foundation models [Bommasani et al. 2021], we propose a comprehensive solution. For human reasoning, we leverage a vision-language model (VLM) to generate initial descriptions of the imaging condition of composite images. To incorporate human priors, we rely on large text-to-image (T2I) generative models trained on extensive natural image datasets, embedding intrinsic knowledge of natural image distribution. We employ text-guided editing technologies as editing tools and use VLM-rendered descriptions as guidance. Inspired by textual inversion technique [Gal et al. 2022], text embeddings are optimized for a more accurate representation of imaging conditions, and we adopt

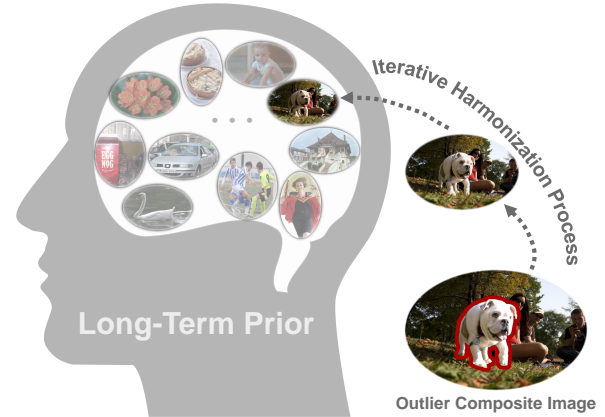


Fig. 2. Human behavior of image harmonization. We humans can perform harmonization relying only on our long-term prior, without seeing many composite images in advance. *E.g.*, to harmonize the overbright dog above.

self-attention maps and edge detection algorithms to ensure structure preservation during editing. For intermediate evaluation, we train a lightweight classifier to assess harmonization levels. The final framework strictly follows human behavior, achieving satisfactory harmonized results. Fig. 1 displays some of our results. In summary, our main contributions are:

- We present a novel perspective on image harmonization aligned with human behavior, exploring image harmonization through a human-centric lens and assessing its feasibility with current technologies.
- We introduce a framework consistent with human behavior, leveraging off-the-shelf VLM and T2I models to achieve satisfactory results without the need for extensive composite image collections. Our designs also handle description inaccuracies, structure distortion, and editing deviation.
- Through experiments across diverse cases, we showcase our method’s visual effectiveness. Comparative user studies with heavily supervised methods underscore the potential of our zero-shot harmonization approach.

2 RELATED WORK

Image harmonization. Compared with traditional methods [Lalonde and Efros 2007; Pitie et al. 2005; Sunkavalli et al. 2010; Xue et al. 2012] that rely on matching low-level statistics between foreground and background, Tsai *et al.* [Tsai et al. 2017] pioneered leveraging deep learning in image harmonization and demonstrated the superiority of its powerful semantic representation capability. To suffice the data-hungry training of deep networks, Cong *et al.* [Cong et al. 2020] constructed a large synthesized image harmonization dataset, by applying a variety of color transforms [Fecker et al. 2008; Lee et al. 2016; Pitié et al. 2007; Reinhard et al. 2001; Xiao and Ma 2006] on segmentation regions of the existing datasets [Bychkovsky et al. 2011; Laffont et al. 2014; Lin et al. 2014]. Many of the following works [Chen et al. 2023c; Cong et al. 2022; Guo et al. 2022; Ke et al. 2022; Sofiiuk et al. 2021; Xue et al. 2022] then based their methods on this large synthesized dataset. Some other approaches have either tried to leverage different transforms [Hang et al. 2022; Jiang et al. 2021; Zhang et al. 2023] or leverage the GAN [Goodfellow et al.

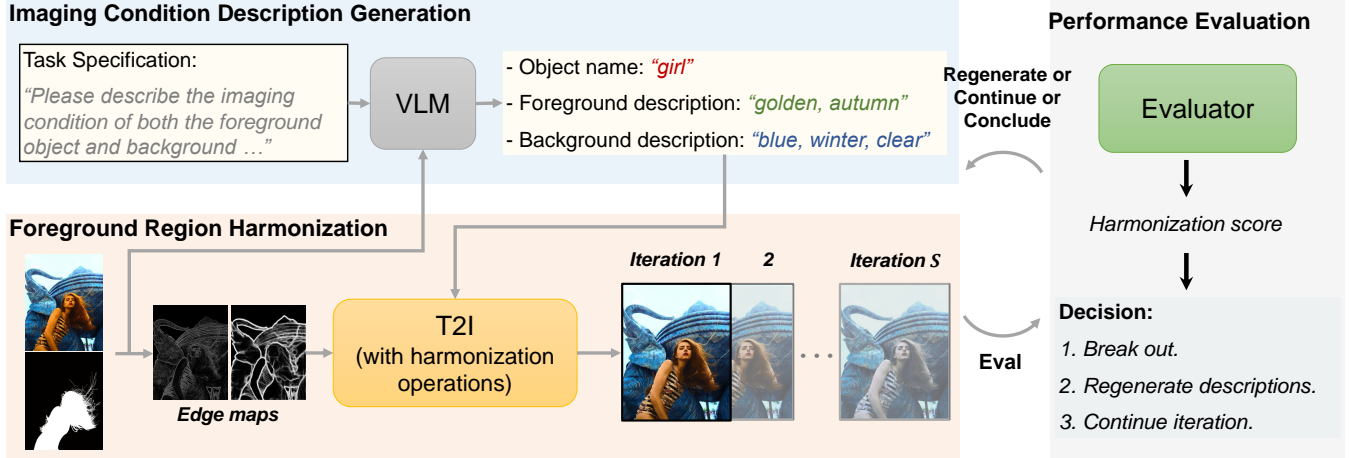


Fig. 3. The proposed framework and workflow across modules. The framework comprises three main components: (a) Imaging Condition Description Generation: A vision-language model (VLM) is utilized to generate descriptions of the input composite image, detailing *what the object is* and *how the foreground and background region are*. (b) Foreground Region Harmonization: A text-to-image (T2I) diffusion generative model is employed, taking both the previously generated descriptions and the edge map of the composite images as input. Image editing technology, together with specific harmonization operations, is used to achieve image harmonization. (c) Performance Evaluation: A two-class classifier serves as an evaluator to determine whether the current result is natural-looking enough or if the description should be regenerated, or if the harmonization iteration should continue.

2014] technique to explore harmonization with unpaired image data [Chen and Kae 2019; Wang et al. 2023; Zhan et al. 2020], but still heavily rely on transforming the segmented regions for composite image collection. Although some promising results have been achieved, whether the synthesized composite images can reflect the real-world situation determines the final generalization and performance of these methods. With more color transformations considered, the trained network can be more robust, yet the training cost also be more unaffordable.

Text-to-image synthesis. Recent advancements in large-scale text-to-image models showcase remarkable generative capabilities. Trained on extensive image-text datasets, these models inherently capture the natural data distribution, enabling them to generate stunning images that align well with given textual guidance. Notably, diffusion models [Ramesh et al. 2022; Rombach et al. 2022; Saharia et al. 2022] have garnered significant attention, leading to their adoption in various downstream applications such as image restoration [Wang et al. 2022] and adversarial attacks [Chen et al. 2023a]. Image editing remains a prevalent application, where these models, guided by text [Ho and Salimans 2021], trained classifiers [Dhariwal and Nichol 2021], and others [Avrahami et al. 2022; Hertz et al. 2022], excel in manipulating local content while preserving the surrounding area. However, these methods are not well-suited for image harmonization, as their primary focus is on altering local content structures.

3 APPROACH

Our method is a fully modularized framework that decomposes the harmonization task into imaging condition description generation, foreground region harmonization, and performance evaluation, as depicted in Fig. 3. Given a composite image, we first generate the description of the imaging condition of the foreground and the background with a vision-language model (VLM). Then, a foreground region harmonization module takes these descriptions, along with

additional edge maps, to harmonize the foreground region through a large text-to-image (T2I) model. The harmonization result is then assessed by an evaluator to make sure the harmonization direction is correct, or the direction gets revised.

3.1 Imaging Condition Description Generation

Recent breakthroughs in large vision-language models, such as Google Gemini and OpenAI GPT-4Vision, have paved the way for significant advancements. Gemini, trained on a massive multi-modality corpus encompassing vision and language, serves as an effective tool for providing descriptions for input composite images, making it an ideal choice for our work.

Our goal with Gemini is twofold. First, we aim to identify the foreground object, such as *dog*, *flower*, etc. Second, we seek descriptions of the imaging conditions for both the foreground and background. Given potential differences in training language corpora between vision-language models (VLM) and text-to-image (T2I) models, some descriptions generated by the VLM may not be accurately interpreted by the T2I model. To address this, we provide a task specification prompt to the VLM, constraining the output scope with environmental text, including *weather*, *season*, *time*, *color tone*, etc.

The input and output of the VLM can be defined as follows:

$$[p_{Obj}, p_{ForeCond}, p_{BackCond}] = \text{VLM}(S, M, I) \quad (1)$$

Here, S represents the task specification prompt, providing an instruction like “Please describe the imaging condition of both the foreground object and background”. Additional details can be found in Appendix B. M and I denote the foreground mask and composite image, respectively. $[p_{Obj}, p_{ForeCond}, p_{BackCond}]$ represent the prompts for the object name, foreground environmental descriptions, and background environmental descriptions, ensuring one or more than one word. An example output could be: [“bird”, “bright orange”, “sunset blue”].

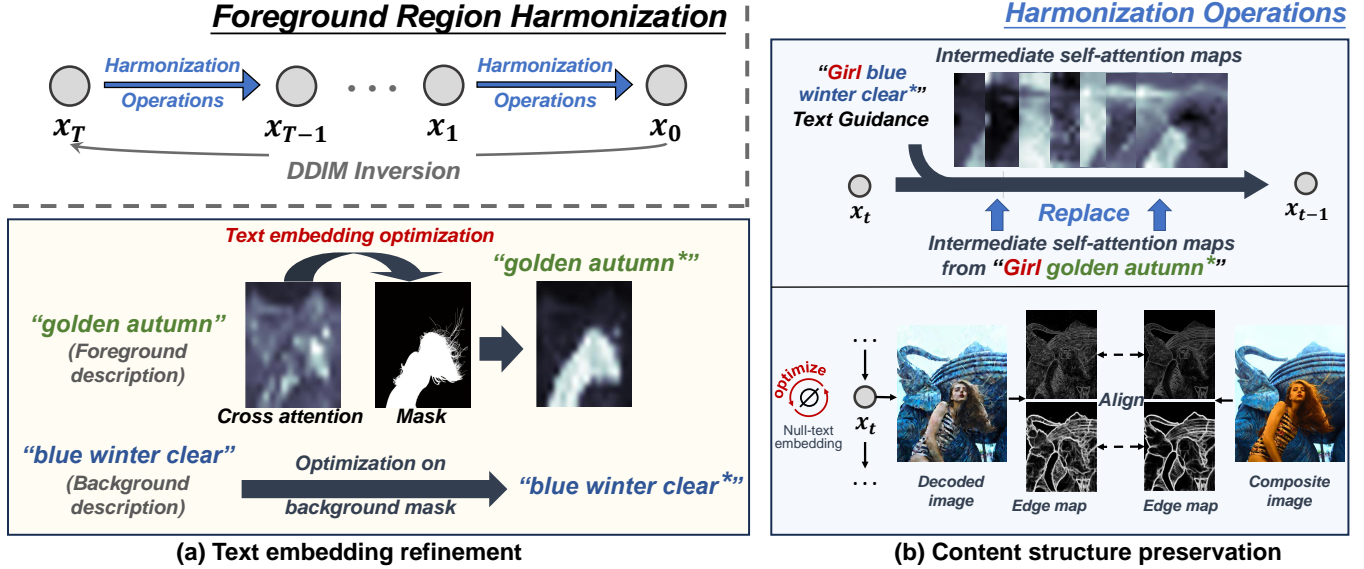


Fig. 4. Designs in the Foreground Region Harmonization. Starting from the composite image, we invert the last harmonized result into its diffusion latent and then employ harmonization operations to obtain the next harmonized result. Among these harmonization operations, (a) Text Embedding Refinement is designed to obtain text embeddings that can better represent the foreground/background environment. (b) In Content Structure Preservation, we leverage self-attention maps to retain high-level structure and utilize edge maps to preserve low-level details. The editing process is achieved based on Prompt-to-Prompt (P2P) editing technology [Hertz et al. 2022]. For brevity, the figure does not explicitly depict this part, and further details can be referred to in their work.

3.2 Foreground Region Harmonization

In our context, the term "human prior" specifically refers to the inherent understanding that humans possess regarding the distribution of natural images. Since our daily experiences predominantly involve realistic and natural scenes, we intuitively internalize this distribution. Similarly, generative models, such as Stable Diffusion [Rombach et al. 2022], are trained on extensive datasets, enabling them to encode knowledge about the natural image distribution in their model weights [Bommasani et al. 2021]. Recognizing these shared characteristics, particularly in modeling the distribution of natural images, we establish a connection between generative models and the human prior and leverage Stable Diffusion in our work.

Foreground Editing. We employ the recent Prompt-to-Prompt (P2P) editing technology [Hertz et al. 2022] to edit the foreground region. Capitalizing on the identified strong correlations between image pixels and text tokens, P2P achieves local image editing by maintaining fixed cross-attention maps while altering prompt texts. For instance, when transforming a *dog* into a *cat*, P2P preserves the original cross-attention map for the *dog* word and simply replaces the guided word with *cat*.

Inspired by P2P, a straightforward approach for image harmonization involves the following steps: Given an input composite image with descriptions of the imaging conditions for both the foreground and background, we initially use DDIM inversion [Song et al. 2020] to project the image into the latent space for P2P utilization. Subsequently, we fix the cross-attention maps for the foreground description and change the guided words from foreground description to background one. The expectation is that the background’s imaging condition description can guide the editing of the foreground region, thereby achieving image harmonization.

However, there exist two challenges in the above approach. Firstly, the provided descriptions of imaging conditions may not accurately represent the foreground and background. For images with rich elements, accurately describing them can be challenging, potentially misleading the T2I model’s editing direction. The second issue is content distortion. P2P, initially designed for modifying object semantics (e.g., changing *dog* to *cat*), does not suit image harmonization well, which focuses on changing color tones without altering object context. Implementing the straightforward solution will result in nontrivial distortions in the foreground content structure.

To address these challenges, we propose an embedding refinement module and a structure preservation module (depicted in Fig. 4). These modules optimize description text embeddings for accurate imaging condition representation and leverage self-attention maps and edge detection algorithms to preserve content structure.

Text Embedding Refinement. In the text-to-image process, Stable Diffusion utilizes text guidance by projecting words into higher-dimensional embeddings. While representing the environment at the word level may pose challenges, finding an accurate high-dimensional representative embedding is more feasible. Drawing from the observed strong correlations between embeddings and image pixels [Hertz et al. 2022], we introduce a quantitative indicator based on cross-attention maps to assess the representativeness of a text embedding in describing the environment: A good description of the imaging condition is characterized by well-focused cross-attention on the target region without overflowing or underfilling. Based on this indicator and inspired by textual inversion technique [Gal et al. 2022], we formulate the optimization objective to refine the embeddings of imaging condition descriptions:

$$\mathcal{L}_{Emb} = \|M - \frac{Att(Emb)}{\max(Att(Emb))}\|_2^2 \quad (2)$$

Here, Emb represents the optimized text embeddings. For multiple embeddings, $Att(Emb)$ is the summation of their cross-attention maps ($Att(Emb) = \sum_{n=1}^N Att(Emb_n)$), M is the background mask, and Att is the cross-attention map between the embedding and image pixels. To align with the value range of the mask, we normalize the attention map with its maximum value. In practice, we utilize the VLM to coarsely describe the imaging condition with some words and then minimize Eq. 2 to obtain a more representative refined embedding. To prevent overfitting, we add a regularization term to ensure the refined embedding is close to its initial state:

$$\min_{Emb} (\mathcal{L}_{Emb} + w \|Emb - Emb_{init}\|_2^2) \quad (3)$$

Here, Emb_{init} is the embedding of the initial text, and w is a hyper-parameter balancing the two terms.

Upon optimizing the text embeddings, we freeze the cross-attention maps of the foreground descriptions and substitute their embeddings with those from the background. However, since there may be a mismatch in the number of embeddings for foreground and background (e.g., 2 for foreground but 3 for background), and different background embeddings may have varying impacts, we replace each foreground embedding with a fusion of background embeddings:

$$Emb_F = \alpha_1 Emb_1 + \alpha_2 Emb_2 + \dots + \alpha_N Emb_N \quad (4)$$

Here, $\alpha_1 + \alpha_2 + \dots + \alpha_N = 1$. The weights $\{\alpha_n\}^N$ are learned during the optimization process of the background descriptions by setting $Att(Emb)$ in Eq. 3 to $\sum_{n=1}^N \alpha_n Att(Emb_n)$. This approach allows the network to determine the importance of each word embedding.

Content Structure Preservation. Directly applying P2P editing technology with the optimized text embeddings may lead to content distortion. To harmonize the image while preserving content structure, we focus on two key aspects.

1) *Self-attention exploitation.* Although P2P [Hertz et al. 2022] has been successful in the local editing of images, we found that even if we changed the text of the environment but not the object itself, the content structure would distort a lot. In contrast to P2P, which relies solely on cross-attention, our approach incorporates additional self-attention maps. Previous studies [Shechtman and Irani 2007; Tumanyan et al. 2022] have shown that self-similarity-based descriptors can capture structure while disregarding appearance information. By initially fixing the self-attention maps in Stable Diffusion for the foreground environment text, we achieve improved content retention. Leveraging the self-attention mechanism, each iteration of editing is effectively constrained to small changes (see Fig. 3), mirroring human behavior.

2) *Edge Detection Constraint.* Given that the self-attention map constraint provides a broad high-level constraint but may not ensure the preservation of finer details, we take an additional step to incorporate fine-grained edge constraints. Specifically, we utilize both a deep edge detection model (Pidinet) [Su et al. 2021] and traditional Sobel kernels [Kanopoulos et al. 1988] to extract edge maps:

$$E_S(I) = (I \otimes K_h + I \otimes K_v) \quad E_D(I) = \text{Pidinet}(I) \quad (5)$$

Here, E_S and E_D represent the Sobel edge map and deep edge map, respectively. K_h and K_v denote horizontal and vertical Sobel kernels, and \otimes signifies convolution.

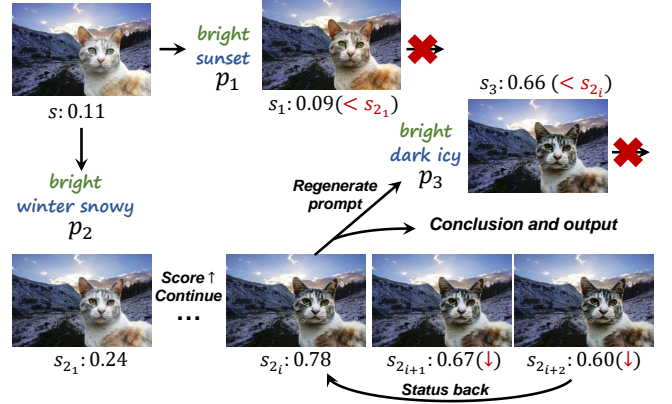


Fig. 5. Demonstration of the evaluation process. We visualize how the decision of Continue/Regenerate/Conclude is made. Please zoom in for a better view.

We implement the constraint by optimizing the unconditional (null-text) embedding of the Stable Diffusion. For each diffusion step, we decode the latent to the image and calculate the loss between the original image’s edge and the resulting image’s edge:

$$\mathcal{L}_{Edge} = \|E_S(I) - E_S(I')\|_2^2 + \gamma \|E_D(I) - E_D(I')\|_2^2 \quad (6)$$

Here, I' denotes the decoded image in the diffusion steps, and γ is a loss weight for balance. For more detailed information on null-text optimization, please refer to [Mokady et al. 2022].

3.3 Performance Evaluation

In the human harmonization process, encountering situations where the result is worse than the initial one after editing is not uncommon. In such cases, a human editor would reassess the evaluate the naturalness of the current result and editing direction.

To replicate this behavior and automate the entire pipeline further, we introduce a two-class classifier to assess the harmonization level of the rendered result. It’s worth noting that this classifier serves as a post-processing step and does not alter the zero-shot nature of the previous harmonization process. Moreover, the classifier incurs minimal computational cost, utilizing significantly fewer images for training compared to previous supervised methods. For instance, training can be completed in just 30 minutes, whereas previous supervised methods may take over 2 days. More detailed information can be found in Appendix C.

The evaluation process is depicted in Fig. 5. At the beginning of harmonization, we use the VLM to generate multiple imaging condition descriptions, denoted as p_1, p_2, \dots, p_K . Each description guides one harmonization iteration, and we pass the results into the classifier, obtaining scores s_1, s_2, \dots, s_K . We select the prompt p_k with the highest score and consistently use it in subsequent iterations. During intermediate harmonization iterations, if the score decreases twice in a row ($s_{k_{i+2}} < s_{k_{i+1}} < s_{k_i}$), we revert to the s_{k_i} state and regenerate the description of the imaging condition to explore whether the new description can guide us to a higher harmonization score. If successful, we continue the harmonization process; otherwise, we conclude the process and output the result with the highest harmonization score as the final outcome.

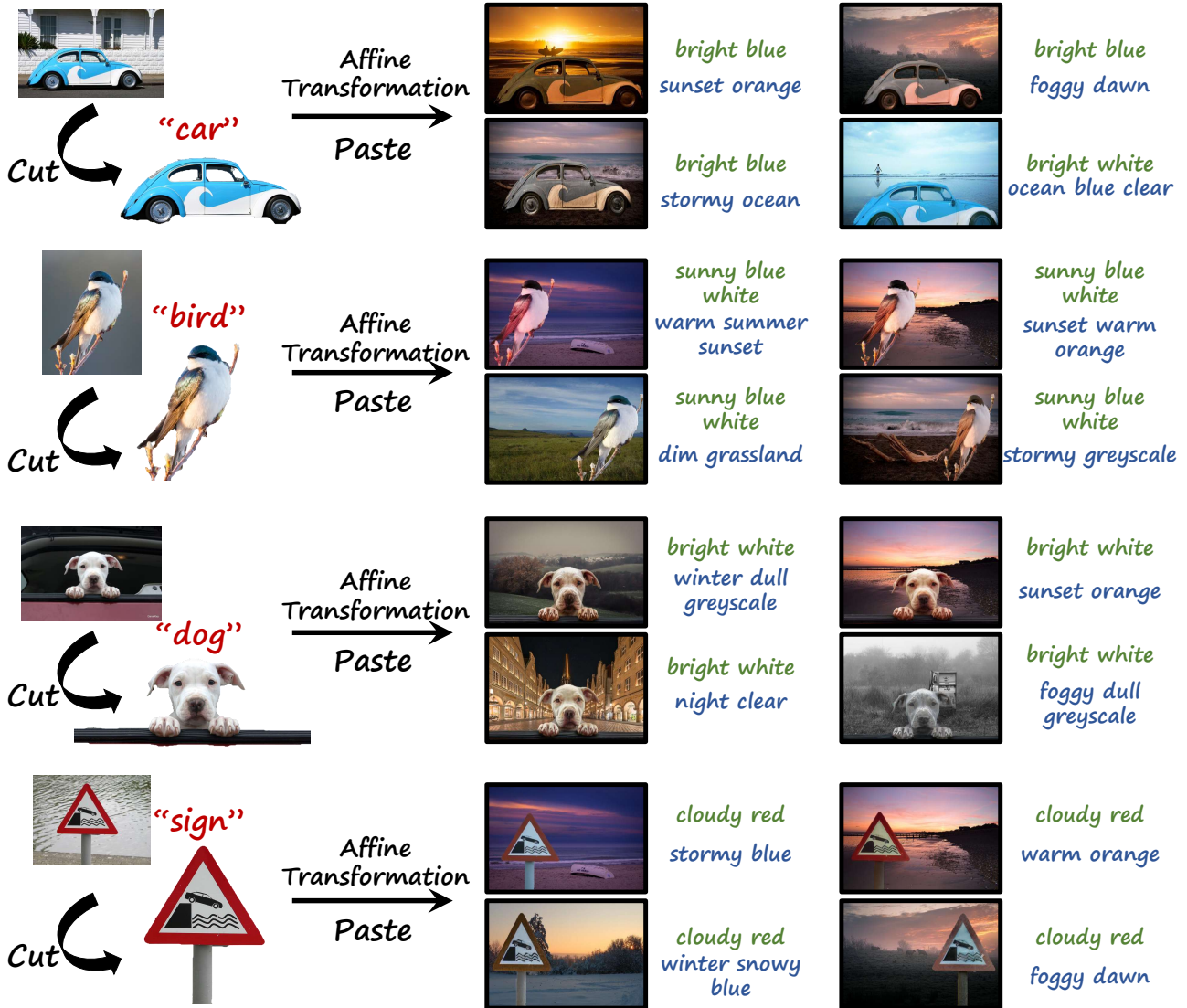


Fig. 6. Qualitative demonstration of our approach’s harmonized results. In the leftmost column, the foreground source image and its extracted foreground object are depicted. The subsequent columns display the harmonized results of the foreground object under various background imaging conditions. The color scheme indicates the object name, descriptions of the foreground imaging condition, and descriptions of the background imaging conditions with **RED**, **GREEN**, and **BLUE**, respectively. Note that multiple prompts may be leveraged in the process, and only the initially chosen description is displayed here.

4 EXPERIMENTS

Here, we present a qualitative demonstration of our method and compare it with supervised harmonization methods. Additional details regarding the implementation, ablation study, and potential applications can be found in Appendix C, D, and E.

4.1 Dataset Setup

To evaluate the effectiveness of our approach in harmonizing real-world composite images, we engaged two image editors to help construct a set of composite images for assessment. Our process involved collecting high-quality images from Flickr, using some as source images for foreground objects and others as source images for the background environment. Various objects, such as humans,

animals, buildings, *etc.*, were extracted from the foreground images and seamlessly integrated into suitable positions in the background image after undergoing transformations like resizing, rotation, and perspective adjustments. In total, we compiled a dataset of 300 composite images for comprehensive evaluation.

4.2 Qualitative Demonstration

We provide qualitative examples of harmonized results across different objects and imaging conditions in Fig. 1, Fig. 6, and Fig. 9. These results showcase the versatility of our approach in effectively handling a variety of real-world composite images. In Fig. 6, it is evident that for the same background image, different descriptions are chosen for different foreground objects, illustrating an adaptive

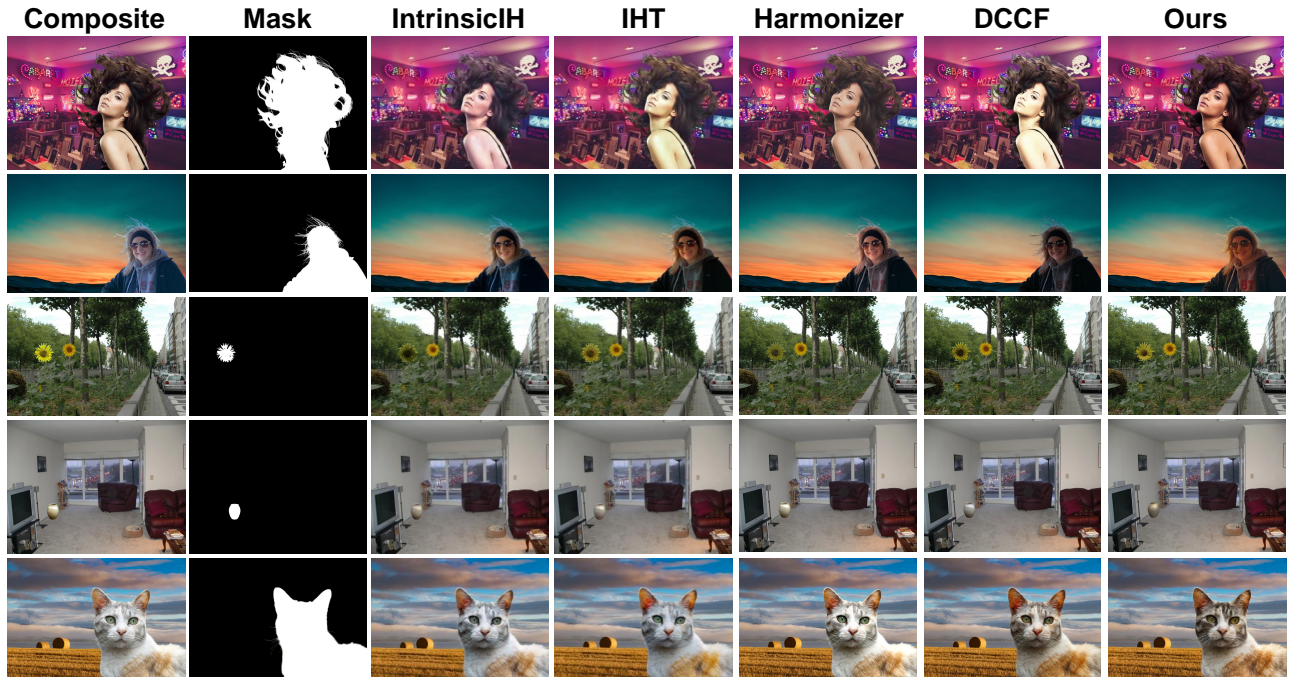


Fig. 7. Comparisons with SOTA harmonization methods. From left to right are composite images, foreground masks, and the harmonized results of Intrinsic [Guo et al. 2021], IHT [Guo et al. 2022], Harmonizer [Ke et al. 2022], DCCF [Xue et al. 2022], and ours.



Fig. 8. Comparisons with SOTA diffusion-based image composition methods. Please zoom in for a better view.

process for selecting more suitable descriptions. These examples highlight the robustness of our approach.

4.3 Human Preference Evaluation

To demonstrate the effectiveness of our approach, we compare it against several popular heavily supervised harmonization methods, including IHT [Guo et al. 2022], DCCF [Xue et al. 2022], Harmonizer [Ke et al. 2022], and Intrinsic [Guo et al. 2021]. The qualitative results are presented in Fig. 7, where our method, even without

relying on heavy training, achieves superior performance to other methods, highlighting the effectiveness of our zero-shot approach.

Additionally, we compare our approach with recent works that leverage diffusion models for image composition tasks. Given their inherent relation to image harmonization, we visualize comparisons with popular methods like AnyDoor [Chen et al. 2023b] and Paint-by-Example [Yang et al. 2023]. From the results in Fig. 8, it's evident that these methods fail to preserve the foreground object's structure, while ours performs better in this aspect.

Table 1. User study. Users are invited to select the more harmonious one between two images. Here, we display the voting percentages of different methods [Guo et al. 2022, 2021; Ke et al. 2022; Xue et al. 2022]. “Comp.” denotes the original composite image.

Comparisons	Voting Rate
Ours v.s. Comp.	89.6%/10.4%
Ours v.s. IntrinsicIH	62.6%/37.4%
Ours v.s. IHT	60.3%/39.7%
Ours v.s. Harmonizer	72.1%/27.9%
Ours v.s. DCCF	70.9%/39.1%

For quantitative comparison, as ground-truth harmonized results are unavailable for these real-world composite images, we follow the approach in [Avrahami et al. 2022; Gal et al. 2022; Mokady et al. 2022; Wu et al. 2022; Xie et al. 2022] and conduct a subjective user study. We invited 40 image editors with more than 2 years of work experience for the study. In each trial, participants were presented with two images, which were either derived from the results of various harmonization methods or represented the original composite image. The display order was randomly shuffled, and participants were required to choose the more harmonious one between the two. A total of 60,000 votes were collected. The vote rates are displayed in Table 1, demonstrating the effectiveness and superiority of our approach.

5 LIMITATION

While our approach offers a modularized framework, it may encounter accumulated errors, such as potential inaccuracies in description generation, deviations in text-to-image editing directions, or inaccuracies in the evaluation classifier. However, this modular design also provides ample room for future improvement. As these networks advance, our techniques should also see improvements due to their modular nature. Another limitation is the time cost associated with our approach. As the diffusion model involves an iterative generation process, our method inherits the drawback of increased time consumption. Additionally, due to the fundamental limitations of the T2I model, despite several designs for structure preservation, there are still deformations in the foreground region, especially in finer details.

6 CONCLUSIONS

In this work, we introduce the feasibility of imitating human behavior and propose a zero-shot image harmonization method. Our approach achieves satisfactory harmonized results without relying on extensive training on a large dataset of composite images. Instead, it leverages the prior knowledge embedded in the pretrained generative model and the guidance of textual descriptions describing the image environment. The effectiveness of our method is demonstrated across a variety of cases. With a fully modularized design, our framework allows for easy integration of future improvements, leveraging the rapid advancements in vision and language models. We hope that our method serves as a stepping stone for

further research and development in the field of zero-shot image harmonization.

REFERENCES

- Omri Avrahami, Dani Lischinski, and Ohad Fried. 2022. Blended diffusion for text-driven editing of natural images. In *Proceedings of the IEEE/CVF Conference on Computer Vision and Pattern Recognition*. 18208–18218.
- Irving Biederman, Robert J Mezzanotte, and Jan C Rabinowitz. 1982. Scene perception: Detecting and judging objects undergoing relational violations. *Cognitive psychology* 14, 2 (1982), 143–177.
- Rishi Bommasani, Drew A Hudson, Ehsan Adeli, Russ Altman, Simran Arora, Sydney von Arx, Michael S Bernstein, Jeannette Bohg, Antoine Bosselut, Emma Brunskill, et al. 2021. On the opportunities and risks of foundation models. *arXiv preprint arXiv:2108.07258* (2021).
- Vladimir Bychkovsky, Sylvain Paris, Eric Chan, and Frédo Durand. 2011. Learning photographic global tonal adjustment with a database of input/output image pairs. In *CVPR 2011*. IEEE, 97–104.
- Bo-Chun Chen and Andrew Kae. 2019. Toward realistic image compositing with adversarial learning. In *Proceedings of the IEEE/CVF Conference on Computer Vision and Pattern Recognition*. 8415–8424.
- Jianqi Chen, Hao Chen, Keyan Chen, Yilan Zhang, Zhengxia Zou, and Zhenwei Shi. 2023a. Diffusion Models for Imperceptible and Transferable Adversarial Attack. *arXiv preprint arXiv:2305.08192* (2023).
- Jianqi Chen, Yilan Zhang, Zhengxia Zou, Keyan Chen, and Zhenwei Shi. 2023c. Dense Pixel-to-Pixel Harmonization via Continuous Image Representation. *arXiv preprint arXiv:2303.01681* (2023).
- Xi Chen, Lianghua Huang, Yu Liu, Yujun Shen, Deli Zhao, and Hengshuang Zhao. 2023b. Anydoor: Zero-shot object-level image customization. *arXiv preprint arXiv:2307.09481* (2023).
- Wenyan Cong, Xinhao Tao, Li Niu, Jing Liang, Xuesong Gao, Qihao Sun, and Liqing Zhang. 2022. High-Resolution Image Harmonization via Collaborative Dual Transformations. In *Proceedings of the IEEE/CVF Conference on Computer Vision and Pattern Recognition*. 18470–18479.
- Wenyan Cong, Jianfu Zhang, Li Niu, Liu Liu, Zhixin Ling, Weiyuan Li, and Liqing Zhang. 2020. Dovenet: Deep image harmonization via domain verification. In *Proceedings of the IEEE/CVF Conference on Computer Vision and Pattern Recognition*. 8394–8403.
- Jodi L Davenport and Mary C Potter. 2004. Scene consistency in object and background perception. *Psychological science* 15, 8 (2004), 559–564.
- Prafulla Dhariwal and Alexander Nichol. 2021. Diffusion models beat gans on image synthesis. *Advances in Neural Information Processing Systems* 34 (2021), 8780–8794.
- Ming Ding, Zhuoyi Yang, Wenyi Hong, Wendi Zheng, Chang Zhou, Da Yin, Junyang Lin, Xu Zou, Zhou Shao, Hongxia Yang, et al. 2021. Cogview: Mastering text-to-image generation via transformers. *Advances in Neural Information Processing Systems* 34 (2021), 19822–19835.
- Ulrich Fecker, Marcus Barkowsky, and André Kaup. 2008. Histogram-based prefiltering for luminance and chrominance compensation of multiview video. *IEEE Transactions on Circuits and Systems for Video Technology* 18, 9 (2008), 1258–1267.
- Weixi Feng, Xuehai He, Tsu-Jui Fu, Varun Jampani, Arjun Akula, Pradyumna Narayana, Sugato Basu, Xin Eric Wang, and William Yang Wang. 2022. Training-Free Structured Diffusion Guidance for Compositional Text-to-Image Synthesis. *arXiv preprint arXiv:2212.05032* (2022).
- Rinon Gal, Yuval Alaluf, Yuval Atzmon, Or Patashnik, Amit H Bermano, Gal Chechik, and Daniel Cohen-Or. 2022. An image is worth one word: Personalizing text-to-image generation using textual inversion. *arXiv preprint arXiv:2208.01618* (2022).
- Ian Goodfellow, Jean Pouget-Abadie, Mehdi Mirza, Bing Xu, David Warde-Farley, Sherjil Ozair, Aaron Courville, and Yoshua Bengio. 2014. Generative Adversarial Nets. In *Advances in Neural Information Processing Systems*, Z. Ghahramani, M. Welling, C. Cortes, N. Lawrence, and K.Q. Weinberger (Eds.), Vol. 27. Curran Associates, Inc. <https://proceedings.neurips.cc/paper/2014/file/5ca3e9b122f61f8f06494c97b1afccf3-Paper.pdf>
- Zonghui Guo, Zhaorui Gu, Bing Zheng, Junyu Dong, and Haiyong Zheng. 2022. Transformer for Image Harmonization and Beyond. *IEEE Transactions on Pattern Analysis and Machine Intelligence* (2022).
- Zonghui Guo, Haiyong Zheng, Yufeng Jiang, Zhaorui Gu, and Bing Zheng. 2021. Intrinsic image harmonization. In *Proceedings of the IEEE/CVF Conference on Computer Vision and Pattern Recognition*. 16367–16376.
- Yucheng Hang, Bin Xia, Wenming Yang, and Qingmin Liao. 2022. SCS-Co: Self-Consistent Style Contrastive Learning for Image Harmonization. In *Proceedings of the IEEE/CVF Conference on Computer Vision and Pattern Recognition*. 19710–19719.
- Amir Hertz, Ron Mokady, Jay Tenenbaum, Kfir Aberman, Yael Pritch, and Daniel Cohen-Or. 2022. Prompt-to-prompt image editing with cross attention control. *arXiv preprint arXiv:2208.01626* (2022).
- Jonathan Ho and Tim Salimans. 2021. Classifier-Free Diffusion Guidance. In *NeurIPS 2021 Workshop on Deep Generative Models and Downstream Applications*.

- Yifan Jiang, He Zhang, Jianming Zhang, Yilin Wang, Zhe Lin, Kalyan Sunkavalli, Simon Chen, Sohrab Amirghodsi, Sarah Kong, and Zhiyang Wang. 2021. Ssh: A self-supervised framework for image harmonization. In *Proceedings of the IEEE/CVF International Conference on Computer Vision*. 4832–4841.
- Nick Kanopoulos, Nagesh Vasanthavada, and Robert L Baker. 1988. Design of an image edge detection filter using the Sobel operator. *IEEE Journal of solid-state circuits* 23, 2 (1988), 358–367.
- Hakki Can Karaimer and Michael S Brown. 2016. A software platform for manipulating the camera imaging pipeline. In *European Conference on Computer Vision*. Springer, 429–444.
- Zhanghan Ke, Chunyi Sun, Lei Zhu, Ke Xu, and Rynson WH Lau. 2022. Harmonizer: Learning to perform white-box image and video harmonization. In *European Conference on Computer Vision*. Springer, 690–706.
- Pierre-Yves Laffont, Zhile Ren, Xiaofeng Tao, Chao Qian, and James Hays. 2014. Transient attributes for high-level understanding and editing of outdoor scenes. *ACM Transactions on graphics (TOG)* 33, 4 (2014), 1–11.
- Jean-Francois Lalonde and Alexei A Efros. 2007. Using color compatibility for assessing image realism. In *2007 IEEE 11th International Conference on Computer Vision*. IEEE, 1–8.
- Joon-Young Lee, Kalyan Sunkavalli, Zhe Lin, Xiaohui Shen, and In So Kweon. 2016. Automatic content-aware color and tone stylization. In *Proceedings of the IEEE conference on computer vision and pattern recognition*. 2470–2478.
- Jingtang Liang, Xiaodong Cun, Chi-Man Pun, and Jue Wang. 2022. Spatial-separated curve rendering network for efficient and high-resolution image harmonization. In *European Conference on Computer Vision*. Springer, 334–349.
- Tsung-Yi Lin, Michael Maire, Serge Belongie, James Hays, Pietro Perona, Deva Ramanan, Piotr Dollár, and C Lawrence Zitnick. 2014. Microsoft coco: Common objects in context. In *European conference on computer vision*. Springer, 740–755.
- Ilya Loshchilov and Frank Hutter. 2017. Decoupled weight decay regularization. *arXiv preprint arXiv:1711.05101* (2017).
- Ron Mokady, Amir Hertz, Kfir Aberman, Yael Pritch, and Daniel Cohen-Or. 2022. Null-text Inversion for Editing Real Images using Guided Diffusion Models. *arXiv preprint arXiv:2211.09794* (2022).
- Francois Pitie, Anil C Kokaram, and Rozenn Dahyot. 2005. N-dimensional probability density function transfer and its application to color transfer. In *Tenth IEEE International Conference on Computer Vision (ICCV'05) Volume 1, Vol. 2*. IEEE, 1434–1439.
- François Pitié, Anil C Kokaram, and Rozenn Dahyot. 2007. Automated colour grading using colour distribution transfer. *Computer Vision and Image Understanding* 107, 1-2 (2007), 123–137.
- Aditya Ramesh, Prafulla Dhariwal, Alex Nichol, Casey Chu, and Mark Chen. 2022. Hierarchical text-conditional image generation with clip latents. *arXiv preprint arXiv:2204.06125* (2022).
- Aditya Ramesh, Mikhail Pavlov, Gabriel Goh, Scott Gray, Chelsea Voss, Alec Radford, Mark Chen, and Ilya Sutskever. 2021. Zero-shot text-to-image generation. In *International Conference on Machine Learning*. PMLR, 8821–8831.
- Erik Reinhard, Michael Adhikhmin, Bruce Gooch, and Peter Shirley. 2001. Color transfer between images. *IEEE Computer graphics and applications* 21, 5 (2001), 34–41.
- Robin Rombach, Andreas Blattmann, Dominik Lorenz, Patrick Esser, and Björn Ommer. 2022. High-resolution image synthesis with latent diffusion models. In *Proceedings of the IEEE/CVF Conference on Computer Vision and Pattern Recognition*. 10684–10695.
- Chitwan Saharia, William Chan, Saurabh Saxena, Lala Li, Jay Whang, Emily Denton, Seyed Kamyar Seyed Ghasemipour, Burcu Karagol Ayan, S Sara Mahdavi, Rapha Gontijo Lopes, et al. 2022. Photorealistic Text-to-Image Diffusion Models with Deep Language Understanding. *arXiv preprint arXiv:2205.11487* (2022).
- Eli Shechtman and Michal Irani. 2007. Matching local self-similarities across images and videos. In *2007 IEEE Conference on Computer Vision and Pattern Recognition*. IEEE, 1–8.
- Konstantin Sofiiuk, Polina Popenova, and Anton Konushin. 2021. Foreground-aware semantic representations for image harmonization. In *Proceedings of the IEEE/CVF Winter Conference on Applications of Computer Vision*. 1620–1629.
- Jiaming Song, Chenlin Meng, and Stefano Ermon. 2020. Denoising diffusion implicit models. *arXiv preprint arXiv:2010.02502* (2020).
- Zhuo Su, Wenzhe Liu, Zitong Yu, Dewen Hu, Qing Liao, Qi Tian, Matti Pietikäinen, and Li Liu. 2021. Pixel difference networks for efficient edge detection. In *Proceedings of the IEEE/CVF international conference on computer vision*. 5117–5127.
- Kalyan Sunkavalli, Micah K Johnson, Wojciech Matusik, and Hanspeter Pfister. 2010. Multi-scale image harmonization. *ACM Transactions on Graphics (TOG)* 29, 4 (2010), 1–10.
- Yi-Hsuan Tsai, Xiaohui Shen, Zhe Lin, Kalyan Sunkavalli, Xin Lu, and Ming-Hsuan Yang. 2017. Deep image harmonization. In *Proceedings of the IEEE Conference on Computer Vision and Pattern Recognition*. 3789–3797.
- Narek Tumanyan, Omer Bar-Tal, Shai Bagon, and Tali Dekel. 2022. Splicing ViT Features for Semantic Appearance Transfer. In *Proceedings of the IEEE/CVF Conference on Computer Vision and Pattern Recognition*. 10748–10757.
- Ke Wang, Michaël Gharbi, He Zhang, Zhihao Xia, and Eli Shechtman. 2023. Semi-supervised Parametric Real-world Image Harmonization. In *Proceedings of the IEEE/CVF Conference on Computer Vision and Pattern Recognition*. 5927–5936.
- Yinhua Wang, Jiwen Yu, and Jian Zhang. 2022. Zero-Shot Image Restoration Using Denoising Diffusion Null-Space Model. *arXiv preprint arXiv:2212.00490* (2022).
- Qiucheng Wu, Yujian Liu, Handong Zhao, Ajinkya Kale, Trung Bui, Tong Yu, Zhe Lin, Yang Zhang, and Shiyu Chang. 2022. Uncovering the Disentanglement Capability in Text-to-Image Diffusion Models. *arXiv preprint arXiv:2212.08698* (2022).
- Xuezhong Xiao and Lizhuang Ma. 2006. Color transfer in correlated color space. In *Proceedings of the 2006 ACM international conference on Virtual reality continuum and its applications*. 305–309.
- Shaoan Xie, Zhifei Zhang, Zhe Lin, Tobias Hinz, and Kun Zhang. 2022. SmartBrush: Text and Shape Guided Object Inpainting with Diffusion Model. *arXiv preprint arXiv:2212.05034* (2022).
- Ben Xue, Shenghui Ran, Quan Chen, Rongfei Jia, Binqiang Zhao, and Xing Tang. 2022. Dccf: Deep comprehensible color filter learning framework for high-resolution image harmonization. In *European Conference on Computer Vision*. Springer, 300–316.
- Su Xue, Aseem Agarwala, Julie Dorsey, and Holly Rushmeier. 2012. Understanding and improving the realism of image composites. *ACM Transactions on graphics (TOG)* 31, 4 (2012), 1–10.
- Binxin Yang, Shuyang Gu, Bo Zhang, Ting Zhang, Xuejin Chen, Xiaoyan Sun, Dong Chen, and Fang Wen. 2023. Paint by example: Exemplar-based image editing with diffusion models. In *Proceedings of the IEEE/CVF Conference on Computer Vision and Pattern Recognition*. 18381–18391.
- Jiahui Yu, Yuanzhong Xu, Jing Yu Koh, Thang Luong, Gunjan Baid, Zirui Wang, Vijay Vasudevan, Alexander Ku, Yinfei Yang, Burcu Karagol Ayan, et al. 2022. Scaling autoregressive models for content-rich text-to-image generation. *arXiv preprint arXiv:2206.10789* (2022).
- Hui Zeng, Jianrui Cai, Lida Li, Zisheng Cao, and Lei Zhang. 2020. Learning image-adaptive 3d lookup tables for high performance photo enhancement in real-time. *IEEE Transactions on Pattern Analysis and Machine Intelligence* (2020).
- Fangneng Zhan, Shijian Lu, Changgong Zhang, Feiying Ma, and Xuansong Xie. 2020. Adversarial image composition with auxiliary illumination. In *Proceedings of the Asian Conference on Computer Vision*.
- Bo Zhang, Yuxuan Duan, Jun Lan, Yan Hong, Huijia Zhu, Weiqiang Wang, and Li Niu. 2023. Controlcom: Controllable image composition using diffusion model. *arXiv preprint arXiv:2308.10040* (2023).
- Bolei Zhou, Hang Zhao, Xavier Puig, Tete Xiao, Sanja Fidler, Adela Barriuso, and Antonio Torralba. 2019. Semantic understanding of scenes through the ade20k dataset. *International Journal of Computer Vision* 127, 3 (2019), 302–321.

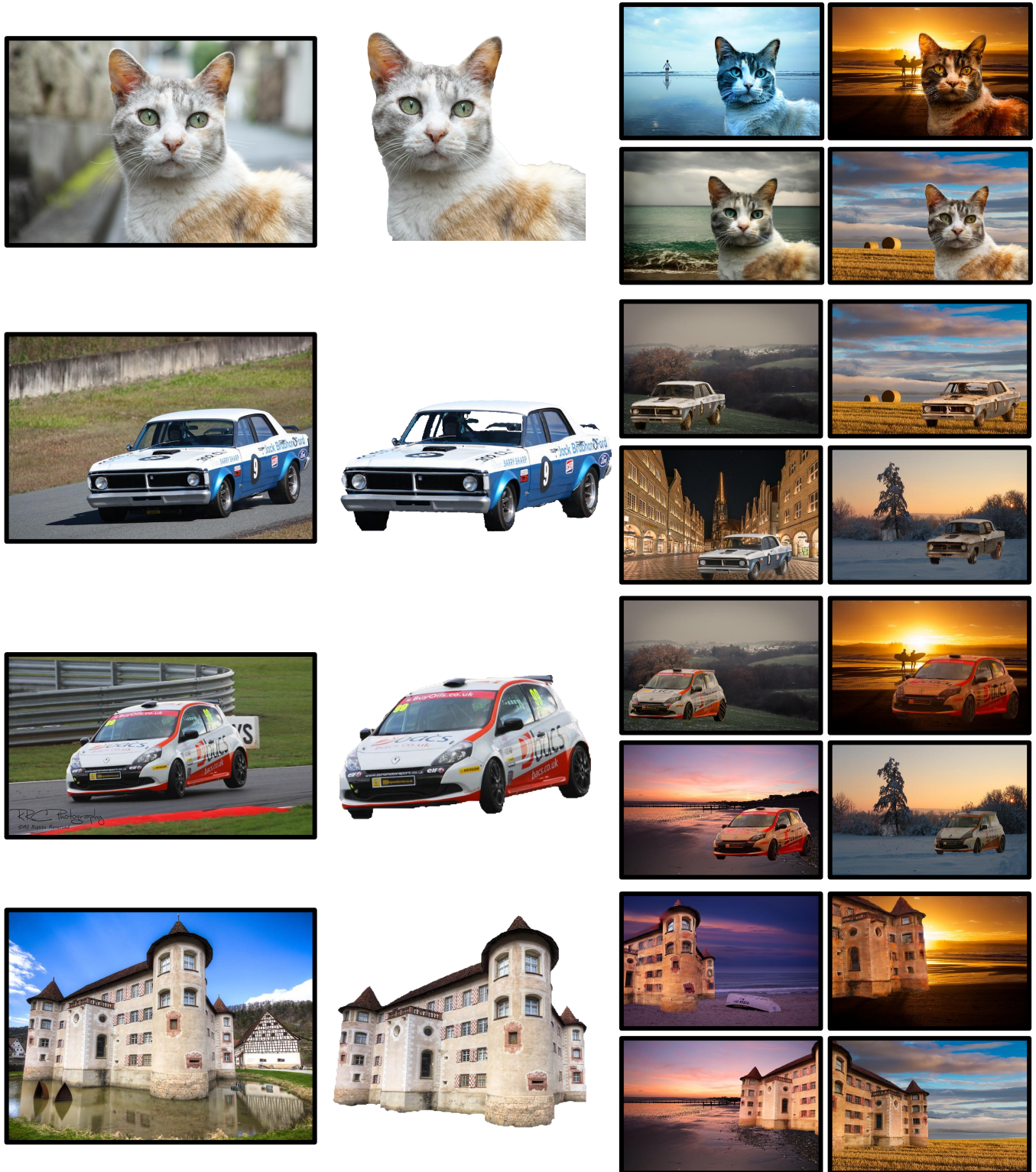


Fig. 9. Additional qualitative demonstration of our approach’s harmonized results. In the left two columns, the foreground source image and its extracted foreground object are depicted. The subsequent columns display the harmonized results of the foreground object under various background imaging conditions.

A OVERVIEW

In this supplementary file, we will begin by presenting the task specification prompt in Appendix B. Following that, we will delve into the implementation details of our proposed method in Appendix C. Subsequently, in Appendix D, we provide an in-depth exploration of ablation studies. Finally, we will investigate some practical applications of our method in Appendix E.

B TASK SPECIFICATION PROMPT

In Fig. 10, the complete prompt for task specification is presented, guiding the Vision-Language Model (VLM) to produce satisfactory results. To address potential disparities in language corpora between the VLM and the T2I model, we encompass the scope of descriptions related to the imaging condition, ensuring easy interpretation by the T2I model.

C IMPLEMENTATION DETAILS

In our approach, we leverage Google Gemini as the VLM. At the beginning of harmonization, we will generate 3 different imaging condition descriptions. We adopt the Stable Diffusion model [Rombach et al. 2022] as the Text-to-Image (T2I) model. The input resolution is set to 512×512 . We utilize the DDIM sampling schedule [Song et al. 2020] for a deterministic diffusion process, configuring the number of diffusion timesteps to 50. In DDIM inversion, we eliminate conditional guidance by setting the guidance scale to 0. Conversely, in the reverse process, the guidance scale in the classifier-free guidance [Ho and Salimans 2021] is set to 2.5.

The refinement of text embedding is based on the cross-attention maps in the diffusion process. We explore two implementations: optimizing style and training style. The former optimizes the text embedding in each diffusion timestep, similar to [Mokady et al. 2022]. In each step, we optimize the embedding multiple times based on the embedding from the last step, obtaining a series of optimized embeddings by the final timestep. In contrast, the latter trains a single embedding. Using all timesteps as a dataset, we iteratively sample a batch to train the embedding. Both implementations yield satisfactory harmonized results, with the optimizing style being the default unless specified. When adopting AdamW [Loshchilov and Hutter 2017] with an initial learning rate of $1e^{-3}$ ($1e^{-2}$ for training style) and setting w in Eq. 3 in the main paper to 5000 (1000 for training style), we optimize two times in each timestep (training for 50 epochs with a batch size of 4). We found that both implementations can achieve satisfactory harmonized results. If not specified, we leverage the optimizing style in the context.

Regarding Pidinet and Sobel kernels, we observe that Pidinet may fail to capture detailed edges compared to Sobel kernels. Therefore, we set the weight γ in Eq. 6 in the main paper as 0.1.

For the performance evaluator, we utilize the ResNet-50 structure. In its training, we use 1000 generated results and invite 2 image editors to score them on a scale from 0 to 1 in 10 ranks (*i.e.*, 0.1, 0.2, ..., 1). These scores serve as soft labels to train a two-class classifier. All experiments are conducted on a single RTX 4090 GPU.

D ABLATION STUDY

Ablation of Text Embedding Refinement. In Fig. 11, we demonstrate the effectiveness of the proposed Text Embedding Refinement module. Without optimization, it can be seen from the attention maps that the initial text fails to well illustrate the environments of foreground/background areas, resulting in a deviated harmonization direction.

Ablation of content retention designs. From Fig. 12, we can observe that with the self-attention and edge maps, the content structure is largely preserved.

Regularization of Text Embedding Refinement. In Eq. 3 of the main paper, we leverage an additional regularization term to restrict the optimization of text embedding. We ablate the regularization in Fig. 13, and the results have demonstrated its effectiveness. With the regularization, the text embedding will not go far away from the initial and thus play a better guiding role.

Prompt text format. Our text prompt is intentionally kept simple, consisting of only a noun for the object name and some adjectives for the imaging conditions. Interestingly, when examining examples from various large-scale text-to-image models [Ding et al. 2021; Ramesh et al. 2022, 2021; Rombach et al. 2022; Saharia et al. 2022; Yu et al. 2022], it is observed that these models often leverage more complete and formal sentences to describe a given image. In an exploration of the impact of different prompt text formats, as illustrated in Fig. 14, we observe that the currently used simplified texts lead to superior results. We attribute this outcome to the potential constraints introduced by longer prompt texts. The use of more extended prompts may introduce additional perturbations in the process, while the simplicity of our text format appears to facilitate the harmonization process significantly.

Prompt text order. Interestingly, we observed that altering the order of prompt texts results in variations in the generated images. Specifically, when the environment text precedes the content text, there is a noticeable decrease in performance, as illustrated in Fig. 14. Upon closer examination of the internal structure of the Stable Diffusion [Rombach et al. 2022], we identified the causal attention mask as a contributing factor. This attention mechanism blends the semantics of the latter text token with the preceding token. Consequently, placing the content text after the environment text makes it susceptible to the optimization process of the preceding environment text. This, in turn, leads to challenges in preserving the content structure. Notably, this observation aligns with the findings reported by [Feng et al. 2022].

E APPLICATIONS

In this subsection, we go a further step to explore the applications of our method. We mainly focus on three: painterly image harmonization, user auxiliary, and multiple instances harmonization.

Painterly image harmonization. Besides the harmonized results on the natural composite images displayed in the main paper, we try to generalize our method to composite images with a large style gap between the foreground and background. Here, we evaluate the performance on some artistic pictures. To achieve better results, we slightly relax the constraint on content retention by utilizing self-attention maps only in certain diffusion timesteps (for

Task Specification

I want to choose some words to describe the composite image, which is made by superimposing cut-out object onto the background image.

This is the composite image: **Insert_Composite_Image**. This is the mask of the foreground object: **Insert_Mask_Image**. The foreground region is the mask region, while the rest constitutes the background.

Here, I provide a set of descriptive words categorized in a dictionary as follows:

{'brightness': [dazzling, bright, dim, dull, shaded, shadowed],
'weather': [cloudy, sunny, rainy, snowy, foggy, windy, stormy, clear, misty],
'temperature': [hot, warm, cool, cold, icy],
'season': [spring, summer, autumn, winter],
'time': [dawn, sunrise, daylight, twilight, sunset, dusk, dark, night],
'color tone': [greyscale, neon, golden, white, blue, green, yellow, orange, red, earthy],
'environment': [city, rural, lake, ocean, mountain, forest, desert, grassland, sky, space, indoor, street]}

Now, I need to first give the name of the foreground object and then select appropriate words from the above dictionary to describe both the foreground object and background.

Here are the specific instructions:

1. Give the name of the foreground object
2. Choose one or more words from the entire dictionary that best describe the style of foreground. (e.g. brightness, color tone...)
3. Choose one or more words from the entire dictionary that best describe the background. (e.g. brightness, weather, temperature, season ...)

Note: The desired output format should be: (foreground object name) X & (foreground) X X ... & (background) X X ..., where X represents a word. For example, dog & (foreground) bright summer & (background) winter dull greyscale (Only for reference format). Ensure adherence to this format in your response; any other formats will not be accepted.

Fig. 10. Task specification used for generating descriptions of object names, foreground imaging conditions, and background imaging conditions employing Google Gemini.

natural images all timesteps are considered). From Fig. 15, it can be seen that our method still succeeds in harmonizing the artwork images. We attribute this success to the powerful generative model

prior. As mentioned in Sec. 1 of the main paper, a human mainly relies on his long-term prior on harmonious images to conduct the image harmonization process, and can often achieve harmonious



Fig. 11. Ablation of the text embedding refinement.



Fig. 12. Ablation of the operations for content structure preservation. We ablate the utilization of self-attention maps and the edge maps here.

results. Similar to that, thanks to the extremely large amount of real-world training data, the pretrained large-scale generative models inherently have that prior. Thus, our method, based on the generative model prior, can gain better generalization to a variety of image types, while the existing approaches [Chen et al. 2023c; Cong et al. 2022; Guo et al. 2022; Hang et al. 2022; Jiang et al. 2021; Ke et al.



Fig. 13. Ablation of the regularization term in the text embedding refinement.



Fig. 14. Ablation of the format and order of the initial text. The effect of formal/simple text is explored, together with whether the environment text is placed at the end. Please zoom in for a better view.

2022; Xue et al. 2022] are limited to be applied to the specific scope of the synthesized composite images seen in their training phase.

User auxiliary. As depicted in Fig. 3 in the main paper, our method is an iterative harmonization process. Each time the composite image is harmonized a little. Thus, compared with the one-step methods [Cong et al. 2020; Guo et al. 2022; Hang et al. 2022; Tsai et al. 2017], the user observes all the intermediate results, which can bring many benefits and leads the method to be a white-box approach. Specifically, due to the trivial content distortion between the results of two adjacent iterations, we can optimize a 3D LUT [Karaimer and Brown 2016; Zeng et al. 2020], which is a lookup table that maps RGB values between two images. By predicting either a global 3D LUT for the entire foreground region or multiple local LUTs for foreground meaningful parts such as faces, we can reveal the latent operations of the model, which in turn can provide guidance for an image editor to harmonize images. The process is illustrated in Fig. 16.



Fig. 17. Pipeline for harmonizing multiple instances.

“Cat/House/Bird/Plane photo*” → painting*



Fig. 15. Further application of painterly image harmonization. We explore generalizing our method on artwork. The small image in the lower left corner of each image is the original composite image. Please zoom in for a better view.

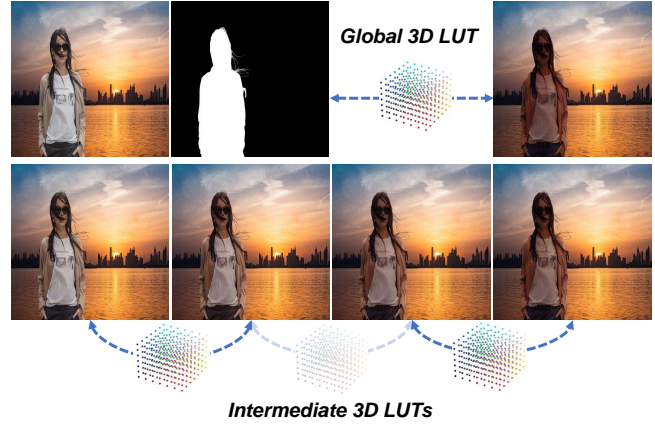


Fig. 16. Further application as user auxiliary. With our iterative harmonization process, the intermediate operation of the network can be extracted and converted to 3D LUTs, which can be leveraged as guidance for the human process.

Multiple instances harmonization. Since we need an initial environmental text for foreground/background, our method may not work well when processing multiple instances simultaneously. However, if we break it down into several separate parts, then we can make it (see Fig. 17). This will not affect the user experience much, as in real-world scenarios, users mostly add foreground instances to the background image one by one.